

Improvement of electroluminescent performance of n-ZnO/AlN/p-GaN light-emitting diodes by optimizing the AlN barrier layer

S. G. Zhang, X. W. Zhang, Z. G. Yin, J. X. Wang, J. J. Dong et al.

Citation: *J. Appl. Phys.* **109**, 093708 (2011); doi: 10.1063/1.3590399

View online: <http://dx.doi.org/10.1063/1.3590399>

View Table of Contents: <http://jap.aip.org/resource/1/JAPIAU/v109/i9>

Published by the [American Institute of Physics](#).

Related Articles

Enhancement of emission characteristics of cadmium-free ZCIS/ZnS/SiO₂ quantum dots by Au nanoparticles
Appl. Phys. Lett. **101**, 041908 (2012)

Emission enhancement in GaN-based light emitting diodes with shallow triangular quantum wells
Appl. Phys. Lett. **101**, 041116 (2012)

Improved quantum efficiency in InGaN light emitting diodes with multi-double-heterostructure active regions
Appl. Phys. Lett. **101**, 041115 (2012)

Ultraviolet electroluminescence from horizontal ZnO microrods/GaN heterojunction light-emitting diode array
Appl. Phys. Lett. **101**, 041110 (2012)

An improved carrier rate model to evaluate internal quantum efficiency and analyze efficiency droop origin of InGaN based light-emitting diodes
J. Appl. Phys. **112**, 023107 (2012)

Additional information on J. Appl. Phys.

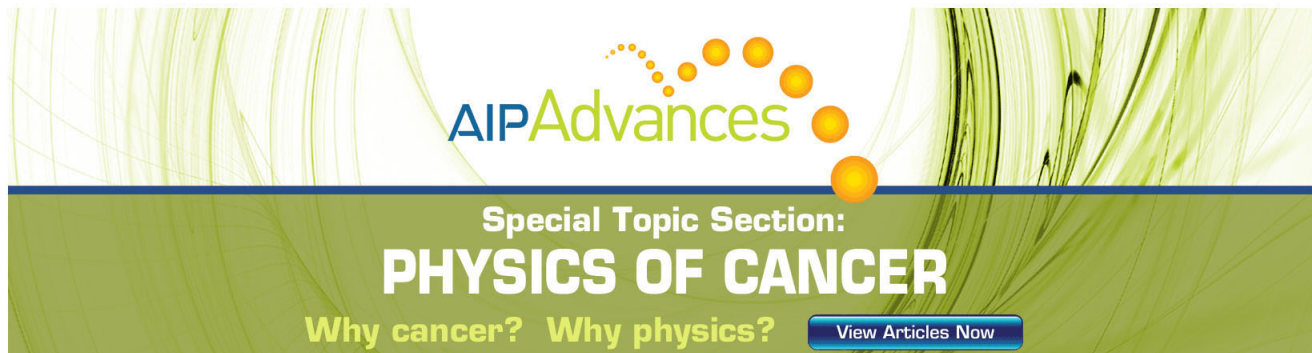
Journal Homepage: <http://jap.aip.org/>

Journal Information: http://jap.aip.org/about/about_the_journal

Top downloads: http://jap.aip.org/features/most_downloaded

Information for Authors: <http://jap.aip.org/authors>

ADVERTISEMENT



AIP Advances

Special Topic Section:
PHYSICS OF CANCER

Why cancer? Why physics? [View Articles Now](#)

Improvement of electroluminescent performance of *n*-ZnO/AlN/*p*-GaN light-emitting diodes by optimizing the AlN barrier layer

S. G. Zhang,¹ X. W. Zhang,^{1,a)} Z. G. Yin,¹ J. X. Wang,² J. J. Dong,¹ Z. G. Wang,¹ S. Qu,^{1,3} B. Cui,⁴ A. M. Wowchak,⁴ A. M. Dabiran⁴ and P. P. Chow⁴

¹Key Lab of Semiconductor Materials Science, Institute of Semiconductors, Chinese Academy of Sciences, Beijing, 100083, People's Republic of China

²Semiconductor Lighting Technology R&D Center, Institute of Semiconductors, CAS, Beijing 100083, People's Republic of China

³Eopilly New Energy Technology Co. Ltd., Jiangsu 226612, People's Republic of China

⁴SVT Associates, Inc., Eden Prairie, Minnesota 55344, USA

(Received 25 February 2011; accepted 9 April 2011; published online 13 May 2011)

The effects of the growth temperature and thickness of AlN layer on the electroluminescence (EL) performance of *n*-ZnO/AlN/*p*-GaN devices have been systematically investigated. It is found that the higher growth temperature of AlN layer (T_{AlN}) may facilitate the improvement of EL performance of the device, which is attributed to that the crystalline quality of AlN layer improves with increasing growth temperatures T_{AlN} . Besides the crystallinity of AlN layer, the thickness of AlN barrier layer plays an important role on the performance of the device. The thinner AlN layer is not enough to cover the whole surface of GaN, while the thicker AlN layer is unfavorable to the tunneling of carriers and many of electrons will be captured and recombined nonradiatively via the deep donors within the thick AlN layer. We have demonstrated that the AlN layer at the growth temperature of 700 °C with an optimized thickness of around 10 nm could effectively confine the injected carriers and suppress the formation of interfacial layer, thus, the EL performance of *n*-ZnO/AlN/*p*-GaN device could be significantly improved. © 2011 American Institute of Physics. [doi:10.1063/1.3590399]

I. INTRODUCTION

Ultraviolet (UV) light emitting diodes (LEDs) are of great interest for their potential application in long-lifetime solid-state lighting, full-color displays, air and water purification and biomedical instrumentation systems.^{1,2} In virtue of the relatively large exciton binding energy (60 meV) and direct wide bandgap (3.37 eV) at room temperature (RT), ZnO has been regarded as one of the most promising candidates for UV LEDs.³⁻⁵ Although ZnO *p*-*n* homojunction LEDs have been fabricated, reliable and reproducible production of *p*-type ZnO films is still challenging due to its self-compensation mechanism which severely constrains the efficiency of ZnO homojunction LEDs.^{6,7} As an intriguing alternative, *p*-*n* heterojunction LEDs with the ZnO as the *n*-type layer has been proposed. In view of the similar properties and excellent lattice matching (1.8%) between ZnO and GaN, the latter appears specially suited for the fabrication of ZnO heterojunction LEDs.⁸ In fact, the heterostructures composed of *n*-ZnO film or nanowires (NWs) on *p*-GaN thin film have been widely investigated recently. Various methods, such as hydrothermal approach and chemical vapor deposition (CVD), have been utilized to fabricate ZnO NWs on GaN substrates, and such devices show obvious blue violet emission due to the confinement effect of NWs and low density of interface defects.⁹⁻¹⁴ Nevertheless, the procedures of fabricating *n*-ZnO NWs/*p*-GaN hybrid LEDs are relatively

complex and cannot be controlled easily. On the other hand, there have been attempts to fabricate *n*-ZnO film/*p*-GaN LEDs, however, the electroluminescence (EL) from the ZnO film/*p*-GaN LEDs is usually weak due to both the unfavorable ZnO/GaN band offsets and the formation of nonradiative centers at the interface. To facilitate carrier confinement and thus, improve the EL performance of the device, wide bandgap materials such as MgO and ZnMgO have been introduced into ZnO film/GaN LEDs.¹⁵⁻¹⁷ It was reported that with the presence of an *i*-MgO layer inserted between the ZnO and GaN layers, the UV emission intensity and output power were much enhanced, while the threshold voltage dropped down to 2.5 V (Ref. 15). The ZnMgO layer was also used to confine the injected carriers and thus increase the intensity of the excitonic emission in the ZnO active region.¹⁶ Moreover, continuous-current-driven lasers in ZnO have been obtained by properly engineering the band alignment of *n*-ZnO/*p*-GaN heterojunctions using a dielectric MgO layer.¹⁷ More recently, we have demonstrated that the EL intensity is greatly enhanced by inserting a thin AlN intermediate layer and it can be attributed to the suppressed formation of the GaO_x interfacial layer and confinement effect rendered by the AlN potential barrier layer.^{18,19} Although rapid progress has been made and even random lasing has been realized for some ZnO-based devices by introducing the potential barrier layer, the effects of the growth conditions of barrier layer on the EL performance of LEDs have not yet been clearly illustrated, which is imperative to develop ZnO-based short-wavelength and high performance optoelectronic devices.

^{a)}Author to whom correspondence should be addressed. Electronic mail: xwzhang@semi.ac.cn.

In this paper, effects of the growth temperature and thickness of AlN layer on the EL performance of *n*-ZnO/AlN/*p*-GaN LEDs have been systematically investigated. It was found that the AlN layer under the growth temperature of 700 °C with an optimized thickness of around 10 nm could effectively confine the injected carriers and suppress the formation of interfacial layer, thus the EL performance of the device could be significantly ameliorated. The thinner AlN layer is not enough to cover the whole surface of GaN, while the thicker AlN layer is unfavorable to the tunneling of carriers and many of electrons will be trapped and nonradiatively recombined via the deep donors within the AlN layer.

II. EXPERIMENTAL DETAILS

The *n*-ZnO/AlN/*p*-GaN heterojunction LEDs were fabricated using a radio-frequency (rf) magnetron sputtering technique. The sputtering chamber was first evacuated to a base pressure of 1.0×10^{-5} Pa, then filled with the working gas to a pressure of 1.0 Pa. The Mg-doped *p*-GaN films grown on *c*-plane sapphire by molecular beam epitaxy (MBE) were used as substrates. The hole concentration and mobility of *p*-GaN were $5.0 \times 10^{17} \text{ cm}^{-3}$ and $15 \text{ cm}^2/\text{V}\cdot\text{s}$, respectively. Prior to deposition, the GaN substrates were sequentially cleaned in the ultrasonic baths of acetone, ethanol and de-ionized water, a 10% HCl/H₂O solution was then utilized to etch the surface of GaN to remove the oxide layer. Finally, the substrates were rinsed with de-ionized water and blown dried with nitrogen gas. For the fabrication of *n*-ZnO/AlN/*p*-GaN LEDs, a AlN barrier layer was firstly deposited by rf sputtering of an Al (99.995%) target in Ar and N₂ mixed ambient (Ar:N₂ = 1:1) on a *p*-GaN layer at various temperatures. Then, a 300 nm ZnO film was deposited by sputtering the ZnO ceramic target (99.999%) at the temperature of 600 °C with a rf power of 80 W. During deposition, the sample holder was rotated to obtain a better uniformity of film. Hall measurements show that the un-doped ZnO films exhibited *n*-type conductivity, and the electron concentration and mobility were $1.5 \times 10^{18} \text{ cm}^{-3}$ and $20 \text{ cm}^2/\text{V}\cdot\text{s}$, respectively. The Au (100nm)/Ni (20nm) and Au (100nm)/Ti (20nm) were successively sputtered as the anode for *p*-GaN and cathode for *n*-ZnO, respectively, and good Ohmic contacts were achieved in both electrodes for all the devices.¹⁸ In order to investigate the effects of the growth conditions of AlN barrier layer on the device performance, two batches of *n*-ZnO/AlN/*p*-GaN LEDs were fabricated in this work. For the first batch of devices, the AlN barrier layers with a fixed thickness of 20 nm were deposited under different growth temperatures (T_{AlN}) ranging from RT to 700 °C. For the second batch of LEDs, the AlN layers with various thicknesses ranging from 5 to 40 nm have been fabricated at a fixed T_{AlN} of 700 °C.

The structure identification of AlN layer was carried out by x-ray diffraction (XRD) in a θ - 2θ mode using a Bruker D8 diffractometer with a Cu K _{α} x-ray source. The cross-sectional interface microstructure of the *n*-ZnO/AlN/*p*-GaN device was studied via transmission electron microscopy (TEM). The surface morphology of AlN film was characterized by atomic force microscopy (AFM) with a NT-MDT

Solver P47 in a semicontact mode. The Keithley 2400 source meter was utilized to measure the current-voltage (*I*-*V*) curves of device. The photoluminescence (PL) measurement was carried out by exciting with a 325 nm He-Cd laser with a power of 30 mW and taken at RT using a photomultiplier tube detector and a grating spectrometer. All the EL spectra of *n*-ZnO/AlN/*p*-GaN LEDs were acquired using a Hitachi F4500 fluorescence spectrometer.

III. RESULTS AND DISCUSSION

The cross-sectional TEM measurement of the *n*-ZnO/AlN/*p*-GaN device has been carried out and the corresponding image is presented in Fig. 1. A three-layer sandwiched structure can be clearly observed with the AlN thickness of around 20 nm. The upper layer of the image reveals a columnar microstructure of the ZnO film. The crystalline nature of ZnO film as well as its orientation was also verified by the [11-20] zone axis selective-area electron diffraction (SAED) pattern taken from the ZnO layer (inset of Fig. 1). Only one set of the diffraction spots was observed and the sharp diffraction spots reflect that the ZnO film is of high crystallinity even with an AlN intermediate layer.

Figure 2 shows the *I*-*V* curves of the *n*-ZnO/AlN/*p*-GaN LEDs with various AlN thicknesses of 10, 30 and 40 nm under the deposition temperature of 700 °C, and the schematic diagram of device is given in the inset of Fig. 2. As can be seen, the clear rectifying behaviors are demonstrated for all the devices. The turn-on voltage of device is defined by extrapolating the linear fit in the high current regions to $I=0$ as indicated by the dashed line in Fig. 2. We can see that the turn-on voltage is as low as 7.5 V under forward bias for the device with a 10 nm AlN layer which is relatively small considering the dielectric nature of the AlN layer. The reverse breakdown voltage is lower than -20 V with the leakage current of 0.2 mA. The series resistance of the LED with the 10 nm AlN layer is comparatively smaller than that of the devices with 30 and 40 nm AlN. The upper results indicate that the device with a 10 nm AlN layer has the optimal electrical properties.

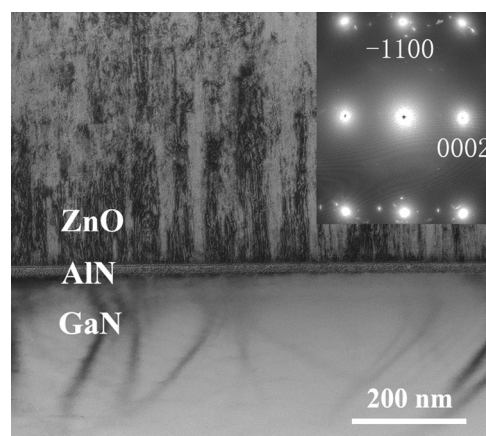


FIG. 1. Cross-sectional TEM image of the *n*-ZnO/AlN/*p*-GaN heterojunction LED, and the [11-20] zone axis SAED pattern recorded from the *n*-ZnO area (inset).

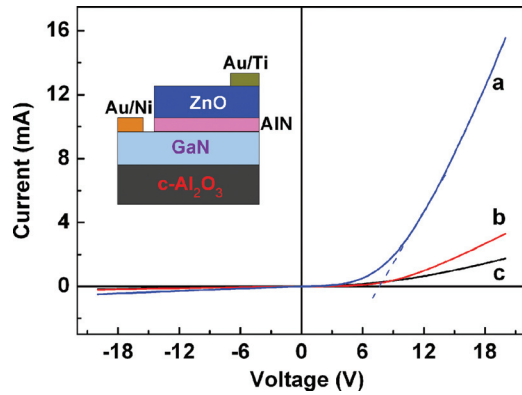


FIG. 2. (Color online) I-V curves of n -ZnO/AlN/ p -GaN LEDs with various AlN thicknesses of (a) 10 nm, (b) 30 nm, and (c) 40 nm. The inset shows the schematic diagram of the device.

Figure 3 presents the RT EL spectrum of n -ZnO/AlN/ p -GaN LED at the injection current of 6 mA, together with the PL spectra of the p -GaN and n -ZnO films, respectively. As can be seen, the RT EL spectrum of the LEDs exhibits a distinct emission peak centered at around 392 nm and a very weak UV emission at 363 nm. The PL spectrum of the Mg-doped GaN film reveals a strong ultraviolet emission peaked at 363 nm corresponding to the band-to-band recombination of GaN (Ref. 20). The PL spectrum of the ZnO film exhibits a sharp peak located at 376 nm associated with the radiative recombination of free and bound excitons, and a broader and weaker green emission related with intrinsic defects.³ The defect-related emission in the visible region is very weak compared with the UV emission for the ZnO film, inferring the low defect density of the as-grown film. It is obvious that the weak EL peak at 363 nm is ascribed to the free exciton recombination from GaN by comparing the EL spectra with PL results. However, neither the main PL peak of ZnO nor GaN matches with the main EL emission peak of device which is located at around 392 nm, thus whether the 392 nm EL emission is originated from ZnO or GaN layer is unclear by simply comparing with the PL spectra. To elucidate such the EL emission, an alternative method is decomposing the EL spectrum into several peaks. For instance, by Gaussian

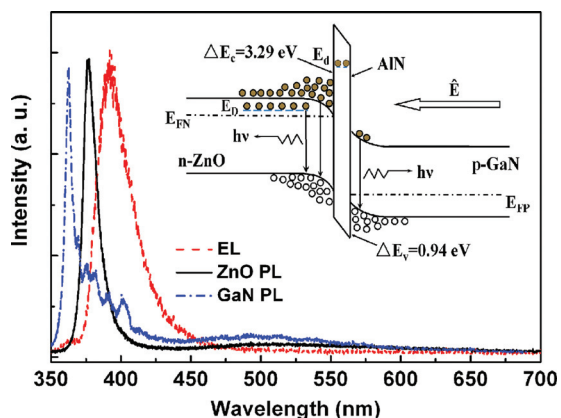


FIG. 3. (Color online) RT EL spectrum of n -ZnO/AlN/ p -GaN LED under the injection current of 6 mA, together with the PL spectra of the p -GaN and n -ZnO films. The inset shows the band alignment diagram of the n -ZnO/AlN/ p -GaN heterojunction under forward bias.

deconvolution of the emission spectrum, the origins of the broad emission at about 405 nm are assigned particularly to three distinct electron hole recombination processes for the n -ZnO/ p -GaN heterojunction LEDs without the barrier layer.¹³ However, the full-width at half maximum (FWHM) of the EL peak at 392 nm is only 27 nm in this work and it is hard to decompose it into different peaks.

The band alignment of heterojunction is an important aspect to consider in studying and determining the originations of EL emissions. The conduction band offset (CBO) between ZnO and AlN and the valence band offset (VBO) between AlN and GaN are experimentally determined to be 3.29 eV and 0.94 eV for the ZnO/AlN/GaN system, respectively.^{18,21} Thus, the energy barrier for electrons (3.29 eV) is much higher than that for holes (0.94 eV) and electrons will be confined in the ZnO layer by the AlN potential barrier layer. On the other hand, because most of the voltage will be applied on the dielectric AlN layer under forward bias, the bands of AlN will bend. The effective barrier in the vicinity of VBO is greatly reduced due to band bending. Consequently, holes in the GaN layer can tunnel through the AlN barrier and enter into the ZnO layer. The electrons in ZnO will recombine with the tunneling holes and the radiative recombination occurs. Therefore, the EL emission peaked at 392 nm could be attributed to the recombination in ZnO layer. The apparent discrepancy in peak position comparing with the PL spectrum of ZnO could be interpreted tentatively in the following. On the one hand, it should be noted that there is some difference between PL and EL processes. The PL process depends on the recombination of nonequilibrium carriers in the surface layer of ZnO films due to the high absorption coefficient of ZnO for the exciting laser beam, whereas, the EL process is determined via the carrier recombination within the space charge region of heterojunctions. Thus, the peak position of EL may be different from that of the PL spectrum even if both of them originate from the radiative recombination from ZnO layer. Actually, the emission at about 400 nm has been observed frequently from the EL spectra of ZnO-based LEDs and is ascribed to the transition from the donors to the valence band or the donor-acceptor pair recombination in ZnO.^{6,17,22}

On the other hand, it has been experimentally and theoretically verified that the unintentionally doped ZnO is n -type and a large number of donor-type defects exist in the ZnO layer.^{3,4} The presence of donor-type defects, E_3 and L_1 , with a level situated around 0.2~0.3 eV below the conduction band has been observed in both single-crystal and polycrystalline ZnO films.^{23,24} Therefore, the 392 nm emission is attributed to the electron transition from the donor-type E_3 or L_1 below the conduction band to the valence band. Furthermore, the AlN layer is not of perfect crystal structure, a small amount of electrons will still tunnel through the AlN layer under forward bias and recombine with holes in GaN layer, which is the origination of the weak 363 nm EL emission. The recombination processes related with the EL emission have been illustrated in terms of the energy band diagram, as presented in the inset of Fig. 3.

Since the improvement of EL performance of n -ZnO/AlN/ p -GaN LED is attributed to inserting a thin AlN intermediate layer,¹⁸ it is reasonable to deduce that the growth

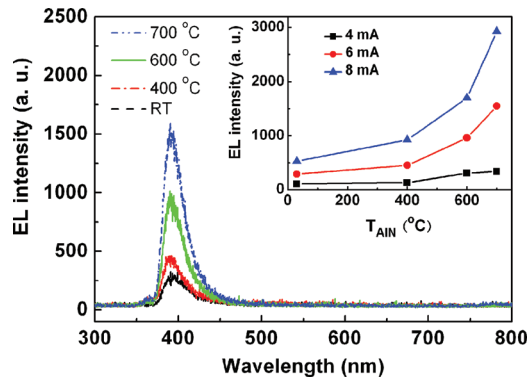


FIG. 4. (Color online) EL spectra of the *n*-ZnO/AlN/*p*-GaN LEDs with the 20 nm AlN layers deposited at different T_{AlN} under the current of 6 mA. The inset shows the dependence of EL intensity on T_{AlN} for various injection currents.

parameters of AlN layer have a close relationship with the EL performance of the device. In order to clarify the effect of T_{AlN} on the EL performance of the device, the LEDs with 20 nm AlN barrier layers deposited at different T_{AlN} have been fabricated, and the corresponding EL spectra at the injection current of 6 mA are shown in Fig. 4. As can be seen, all the EL spectra of the LEDs exhibit a distinct emission peak centered at around 392 nm and a very weak UV emission at 363 nm. The most important feature presented in Fig. 4 is that the 392 nm EL emission exhibits a significant increase in intensity with increasing T_{AlN} . To clearly demonstrate the effects of T_{AlN} on the EL performance, the dependence of EL intensity on T_{AlN} for various injection currents is shown in the inset of Fig. 4. It can be seen that with increasing T_{AlN} the EL intensities increase monotonically for all the injection currents, and the EL intensities approach their maximum at T_{AlN} of 700°C. Obviously, the higher T_{AlN} may facilitate the improvement in the EL performance of the device. We expect that the EL performance of the device will further be improved when T_{AlN} increases to above 700°C, however, it is beyond our experimental conditions.

To shed further light on the role of T_{AlN} in the EL performance, the structure of AlN layer deposited at various T_{AlN} was characterized by XRD measurements. In order to obtain better signal-to-noise ratio of XRD measurements, the AlN films with the thickness of 250 nm were deposited on *p*-GaIn/sapphire (0001) substrates under different T_{AlN} . Figure 5 shows the θ - 2θ XRD patterns of the AlN films at T_{AlN} ranging from RT to 700°C. As can be seen, except for the diffraction peaks centered at 41.65°, 34.60° and 72.98°, corresponding to the *c*-plane reflections of the sapphire (0006), GaN (0002) and GaN (0004), respectively, only the AlN (0002) and (0004) peaks could be observed at 36.02° and 76.50°. It reveals that the AlN films are *c*-axis oriented, with the epitaxial relationship of AlN (0002)||GaN (0002)||sapphire (0002). To further study the crystallinity of AlN films, the x-ray rocking curve of AlN (0002) reflection was acquired (not shown here). The FWHM of AlN (0002) rocking curve is about 0.32° for the AlN film deposited at 700°C, which is relatively small comparing with the other report using the same fabrication method.²⁵ It can be explicitly observed from Fig. 5 that the intensity of AlN (0002)

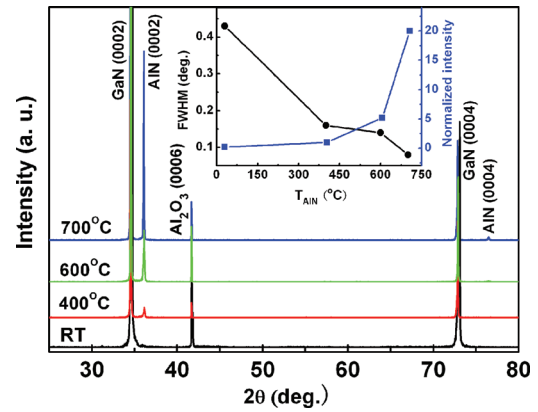


FIG. 5. (Color online) XRD patterns of the AlN films deposited on *p*-GaIn/sapphire substrates at RT, 400, 600 and 700°C, respectively. The inset shows the temperature dependence of the FWHM value and the normalized intensity of AlN (0002) XRD peak for these AlN films.

peak shows a sharply upward trend with increasing T_{AlN} . To demonstrate this variation, the temperature dependence of the normalized XRD intensity is presented in the inset of Fig. 5. It can be seen that the intensity of AlN (0002) peak increases remarkably with increasing T_{AlN} , and the peak intensity of AlN film at 700°C is several orders of magnitude larger than that of sample at RT. Furthermore, the FWHM values of AlN (0002) peak are extracted from the XRD patterns and the temperature dependence of the FWHM for these AlN films is also shown in the inset of Fig. 5. The FWHM of the XRD peak decreases with the increase in T_{AlN} , to a minimum value of 0.08° for the AlN film grown at 700°C. These results indicate that T_{AlN} plays a significant role in determining the crystalline quality of AlN films, and the highest crystallinity of AlN film is obtained at T_{AlN} of 700°C. Comparing with the EL spectra in Fig. 4, we propose that the enhancement of EL intensity with increasing T_{AlN} is associated with the better crystalline quality of AlN barrier layer at the higher temperatures. On the one hand, the higher crystalline quality is in favor of the suppressed formation of GaO_x interfacial layer and confinement effect, which leads to the improved EL performance. On the other hand, the higher crystallinity of AlN layer may also facilitate the epitaxial growth of the subsequent ZnO film.

Besides the crystallinity of AlN layer, the thickness of AlN barrier layer plays an important role on the performance of *n*-ZnO/AlN/*p*-GaIn LEDs since the tunneling probability of carriers is closely associated with the thickness of the barrier layer. In order to evaluate the effects of thickness of AlN barrier layer on the EL performance of the device, the *n*-ZnO/AlN/*p*-GaIn LEDs with various AlN thicknesses ranging from 5 to 40 nm have been fabricated and their EL spectra at the injection current of 8 mA are shown in Fig. 6. The device with a 5 nm AlN layer exhibits a weak emission peak at 392 nm, the EL emission increases distinctly when the AlN thickness increases to 10 nm, with the intensity seven times higher than that of the device with a 5 nm AlN. The intensity of EL emission initiates to decrease for the device with a 15 nm AlN layer, and a weak and broad defect-related emission band at around 500 nm occurs simultaneously. When the thickness of the AlN layer increases further to 30

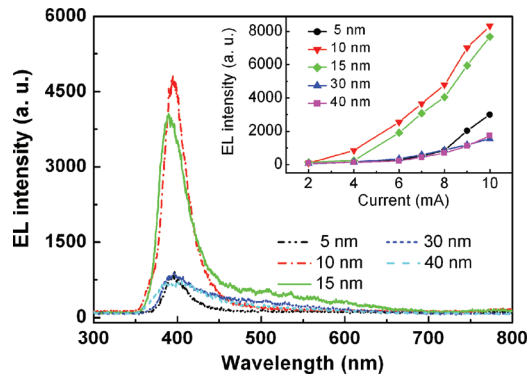


FIG. 6. (Color online) EL spectra of the n -ZnO/AlN/ p -GaN LEDs with various AlN thicknesses under the injection current of 8 mA. The inset shows the injection current dependences of the EL intensity for the n -ZnO/AlN/ p -GaN devices with various AlN thicknesses.

or 40 nm, the performance of the device is degraded, and the EL intensity decreases to the original level of the device with the 5 nm AlN layer. The injection current dependences of the EL intensity for the n -ZnO/AlN/ p -GaN devices with various AlN thicknesses are illustrated in the inset of Fig. 6. The EL intensities are considerably higher for the devices with the 10 or 15 nm AlN layer at all the injection currents, and the EL intensities are low even at the higher injection currents for the other devices. It can be concluded from the above results that the EL intensity obtains its maximum value for the device with the 10 nm AlN potential barrier layer.

It is easy to understand that the performance of the n -ZnO/AlN/ p -GaN device will be deteriorated when the AlN barrier layer is thicker. The thicker AlN layer will reduce the tunneling probability of carriers due to increasing width of potential barrier. As a result, holes cannot tunnel through the AlN barrier layer directly and then the radiative recombination in ZnO will be limited. In this case, a great deal of electrons will be captured by the deep donors in the thick AlN layer and recombined nonradiatively via these defects, since many of the deep donors such as the nitrogen vacancies (V_N) have been recognized in the AlN films.²⁶ Therefore, the EL performance of the device with the thicker AlN layer is greatly limited. As described above, the device with the 5 nm AlN layer exhibits a weak EL emission, which can be understood well by examining the surface morphology of AlN films, as shown in Fig. 7. As can be seen from Fig. 7(a),

though the surface of the 5 nm AlN is relatively flat and the root mean square (RMS) roughness is only 1.4 nm, we can notice that the nanoparticles are loosely packed which means that the 5 nm AlN film is composed of discontinuous nanoparticles. On the other hand, the surface of the 15 nm AlN film is comparatively compact and the nanoparticles are packed tightly, as presented in Fig. 7(b). It is obvious that the 5 nm AlN film is not thick enough to cover the whole GaN surface and parts of the subsequent ZnO film might directly contact with the GaN substrate. Under such circumstances, electrons can drift from ZnO to GaN through these contact-areas under forward bias and the confinement effect of the AlN barrier layer is significantly weakened. Moreover, the direct contact between ZnO and GaN may lead to the formation of GaO_x interfacial layer, which may degrade the EL performance of the device by providing a high density of interface states acting as the nonradiative recombination centers.^{18,27,28} Therefore, the ideal interfacial characteristics and the confinement effect rendered by the AlN layer with the suitable thickness lead to the improved EL performance of the n -ZnO/AlN/ p -GaN LEDs.

IV. CONCLUSION

In summary, the ZnO-based heterojunction LEDs with the AlN barrier layer have been fabricated on the p -GaN/sapphire substrates. The effects of the growth temperature and thickness of the AlN layer on the EL performance of the n -ZnO/AlN/ p -GaN devices have been systematically investigated. On the one hand, the crystalline quality of AlN layer improves with increasing growth temperatures T_{AIN} , and the enhancement of the EL intensity with T_{AIN} is attributed to the better crystalline quality of AlN barrier layer. On the other hand, the thinner AlN layer is not enough to cover the whole surface of GaN, while the thicker AlN layer is unfavorable to the tunneling of carriers and many of electrons will be captured and nonradiatively recombined via the deep donors within the thick AlN layer. We have demonstrated that the optimal EL performance was obtained for the device with a 10 nm AlN layer deposited at T_{AIN} of 700 °C, which can effectively confine the injected carriers and suppress the formation of interfacial layer. These results are useful for the development of high-efficiency ZnO-based LEDs, and may also be helpful in understanding the effects of the AlN potential barrier layer.

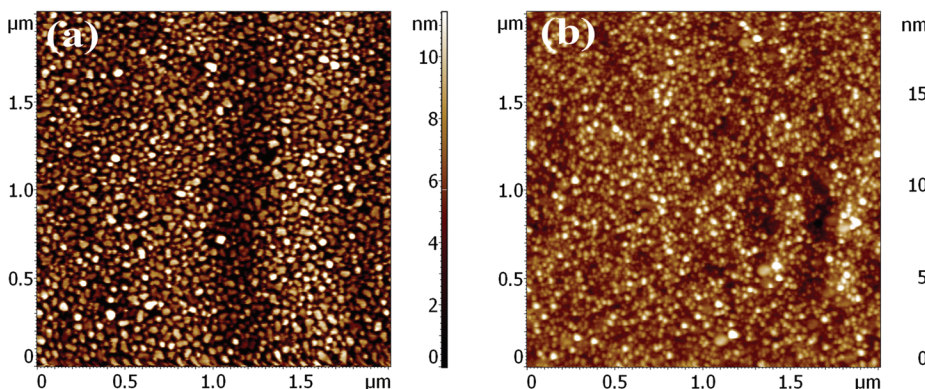


FIG. 7. (Color online) AFM images of the AlN film with the thickness of (a) 5 nm and (b) 15 nm deposited on the p -GaN/sapphire substrates.

ACKNOWLEDGMENTS

This work was financially supported by the “863” Project of China (Grant No. 2009AA03Z305), the National Natural Science Foundation of China (Grant Nos. 60876031 and 60806044) and the National Basic Research Program of China (Grant No. 2010CB933800). The authors are appreciative to Mr. X. Q. He from the Institute of Physics, Chinese Academy of Sciences for his assistance in the TEM measurements.

- ¹J. H. Lim, C. K. Kang, K. K. Kim, I. K. Park, D. K. Hwang, and S. J. Park, *Adv. Mater.* **18**, 2720 (2006).
- ²A. Khan, K. Balakrishnan, and T. Katona, *Nat. Photonics* **2**, 77 (2008).
- ³Ü. Özgür, Ya. I. Alivov, C. Liu, A. Teke, M. A. Reshchikov, S. Dogan, V. Avrutin, S. J. Cho, and H. Morkoc, *J. Appl. Phys.* **98**, 041301 (2005).
- ⁴D. C. Look and B. Claffin, *Phys. Status Solidi B* **241**, 624 (2004).
- ⁵D. K. Hwang, M. S. Oh, J. H. Lim, and S. J. Park, *J. Phys. D: Appl. Phys.* **40**, R387 (2007).
- ⁶A. Tsukazaki, T. Onuma, M. Ohtani, T. Makino, M. Sumiya, K. Ohtani, S. F. Chichibu, S. Fuke, Y. Segawa, H. Ohno, H. Koinuma, and M. Kawasaki, *Nature Mater.* **4**, 42 (2005).
- ⁷X. W. Sun, B. Ling, J. L. Zhao, S. T. Tan, Y. Yang, Y. Q. Shen, Z. L. Dong, and X. C. Li, *Appl. Phys. Lett.* **95**, 133124 (2009).
- ⁸Ya. I. Alivov, J. E. Van Nostrand, D. C. Look, M. V. Chukichev, and B. M. Ataev, *Appl. Phys. Lett.* **83**, 2943 (2003).
- ⁹M. C. Jeong, B. Y. Oh, M. H. Ham, S. W. Lee, and J. M. Myoung, *Small* **3**, 568 (2007).
- ¹⁰J. J. Cole, X. Y. Wang, R. J. Knuesel, and H. O. Jacobs, *Nano Lett.* **8**, 1477 (2008).
- ¹¹H. K. Fu, C. L. Cheng, C. H. Wang, T. Y. Lin, and Y. F. Chen, *Adv. Funct. Mater.* **19**, 3471 (2009).
- ¹²O. Lupan, T. Pauporte, and B. Viana, *Adv. Mater.* **22**, 3298 (2010).
- ¹³S. Xu, C. Xu, Y. Liu, Y. F. Hu, R. Yang, Q. Yang, J. H. Ryou, H. J. Kim, Z. Lochner, S. Choi, R. Dupuis, and Z. L. Wang, *Adv. Mater.* **22**, 4749 (2010).
- ¹⁴O. Lupan, T. Pauporte, B. Viana, I. M. Tiginyanu, V. V. Ursaki, and R. Cortes, *ACS Applied Materials & Interfaces* **2**, 2083 (2010).
- ¹⁵S. Z. Li, G. J. Fang, H. Long, X. M. Mo, H. H. Huang, B. Z. Dong, and X. Z. Zhao, *Appl. Phys. Lett.* **96**, 201111 (2010).
- ¹⁶J. W. Sun, Y. M. Lu, Y. C. Liu, D. Z. Shen, Z. Z. Zhang, B. H. Li, J. Y. Zhang, B. Yao, D. X. Zhao, and X. W. Fan, *J. Phys. D: Appl. Phys.* **41**, 155103 (2008).
- ¹⁷H. Zhu, C. X. Shan, B. Yao, B. H. Li, J. Y. Zhang, Z. Z. Zhang, D. X. Zhao, D. Z. Shen, X. W. Fan, Y. M. Lu, and Z. K. Tang, *Adv. Mater.* **21**, 1613 (2009).
- ¹⁸J. B. You, X. W. Zhang, S. G. Zhang, J. X. Wang, Z. G. Yin, H. R. Tan, W. J. Zhang, P. K. Chu, B. Cui, A. M. Wowchak, A. M. Dabiran, and P. P. Chow, *Appl. Phys. Lett.* **96**, 201102 (2010).
- ¹⁹S. G. Zhang, X. W. Zhang, J. X. Wang, J. B. You, Z. G. Yin, J. J. Dong, B. Cui, A. M. Wowchak, A. M. Dabiran, and P. P. Chow, *Physica Status Solidi-Rapid Research Letters* **5**, 74 (2011).
- ²⁰U. Kaufmann, M. Kunzer, H. Obloh, M. Maier, Ch. Manz, A. Ramakrishnan, and B. Santic, *Phys. Rev. B* **59**, 5561 (1999).
- ²¹T. D. Veal, P. D. C. King, S. A. Hatfield, L. R. Bailey, C. F. McConville, B. Martel, J. C. Moreno, E. Frayssinet, F. Semond, and J. Zúñiga-Pérez, *Appl. Phys. Lett.* **93**, 202108 (2008).
- ²²Y. S. Choi, J. W. Kang, D. K. Hwang, and S. J. Park, *IEEE Trans. Electron Devices* **57**, 26 (2010).
- ²³F. D. Auret, S. A. Goodman, M. J. Legodi, W. E. Meyer, and D. C. Look, *Appl. Phys. Lett.* **80**, 1340 (2002).
- ²⁴A. E. Rakhshani, J. Kokaj, J. Mathew, and B. Peradeep, *Appl. Phys. A* **86**, 377 (2006).
- ²⁵G. F. Iriarte, J. G. Rodriguez, and F. Calle, *Mater. Res. Bull.* **45**, 1039 (2010).
- ²⁶V. A. Soltamov, I. V. Ilyin, A. A. Slotamova, E. N. Mokhov, and P. G. Baranov, *J. Appl. Phys.* **107**, 113515 (2010).
- ²⁷J. Y. Lee, J. H. Lee, H. S. Kim, C. H. Lee, H. S. Ahn, H. K. Cho, Y. Y. Kim, B. H. Kong, and H. S. Lee, *Thin Solid Films* **517**, 5157 (2009).
- ²⁸H. C. Chen, M. J. Chen, M. K. Wu, W. C. Li, H. L. Tsai, J. R. Yang, H. Kuan, and M. Shiojiri, *IEEE J. Quantum Electron.* **46**, 265 (2010).